TM-wave radiation from flanged parallel plate into dielectric slab

J.W. Lee
H.J. Eom
J.H. Lee

Indexing terms: Antenna coupling, Mode matching, Waveguide coupling

Abstract: Flanged parallel-plate radiation of a TM-wave into a dielectric slab is investigated. The Fourier transform is used to represent the radiation field in the spectral domain and the boundary conditions are enforced to obtain the reflection coefficient in rapidly converging series form. Numerical computations are performed to illustrate the radiation behaviour in terms of aperture size, frequency, and slab geometry. It is found that a single-mode approximate solution predicts well the radiation behaviour when a flanged rectangular waveguide is excited in the TE_{10} mode.

1 Introduction

The aperture-antenna radiation into a dielectric slab is an important subject owing to its practical applications to radomes and spacecraft antennas on re-entry vehicles. A considerable amount of investigation has been done to understand its radiation behaviour; for example, the work in [1–3] deals with radiation of aperture antenna when the antenna aperture is attached to a single dielectric slab. The radiation characteristics of the rectangular-slot antenna into stratified media are studied in [4] using the variational technique. *TEM*-wave reflection of a parallel-plate waveguide from a dielectric slab displaced from the waveguide aperture is studied in [5] using wedge diffraction and ray-tracing techniques. In this paper we re-visit the *TM*-wave radiation from a flanged parallel plate into a dielectric slab that is displaced from the antenna aperture. We use the Fourier transform and the mode-matching technique to represent the radiation field in rapidly converging series. Residue calculus is used to perform the branch-cut integration, yielding the reflection coefficient in computationally efficient form.

2 TM-wave analysis

Consider a flanged parallel plate radiating into a dielectric slab, Fig. 1. Regions I, II, III, and IV, respectively, denote the halfspace (wave number $k_1 = \omega\sqrt{[\mu\epsilon_0\epsilon_1]} = 2\pi/\lambda_1$), the dielectric slab (wave number $k_2 = \omega\sqrt{[\mu\epsilon_0\epsilon_2]} = 2\pi/\lambda_2$), the background medium (wave number $k_3 = \omega\sqrt{[\mu\epsilon_0\epsilon_3]} = 2\pi/\lambda_3$), and the aperture (wave number $k_4 = \omega\sqrt{[\mu\epsilon_0\epsilon_4]} = 2\pi/\lambda_4$). Assume that a transverse magnetic (TM) wave to the z-axis H_y^i is incident on a dielectric slab. A time-harmonic factor $e^{-i\omega t}$ is suppressed throughout. In region I the total H-field is

$$H_y^I(x,z) = \frac{1}{2\pi}\int_{-\infty}^{\infty} \tilde{H}_I(\zeta)e^{-i\zeta x + i\kappa_1 z}d\zeta \tag{1}$$

where $\kappa_1 = \sqrt{[k_1^2 - \zeta^2]}$, and $\tilde{H}_I(\zeta)e^{i\kappa_1 d_2}$ and $H_y^I(x, d_2)$ are the Fourier transform pair. In region II the total H-field is

$$H_y^{II}(x,z) = \frac{1}{2\pi}\int_{-\infty}^{\infty} [\tilde{H}_{II}^{+}(\zeta)e^{i\kappa_2 z} + \tilde{H}_{II}^{-}(\zeta)e^{-i\kappa_2 z}]e^{-i\zeta x}d\zeta \tag{2}$$

where $\kappa_2 = \sqrt{[k_2^2 - \zeta^2]}$. In region III the total H-field is

$$H_y^{III}(x,z) = \frac{1}{2\pi}\int_{-\infty}^{\infty} [\tilde{H}_{III}^{+}(\zeta)e^{i\kappa_3 z} + \tilde{H}_{III}^{-}(\zeta)e^{-i\kappa_3 z}]e^{-i\zeta x}d\zeta \tag{3}$$

where $\kappa_3 = \sqrt{[k_3^2 - \zeta^2]}$. In region IV ($-a < x < a$) the total incident and reflected fields are

$$H_y^i(x,z) = \cos a_p(x+a)e^{i\xi_p z} \tag{4}$$

$$H_y^r(x,z) = \sum_{m=0}^{\infty} c_m \cos a_m(x+a)e^{-i\xi_m z} \tag{5}$$

where $\xi_m = \sqrt{[k_4^2 - a_m^2]}$ and $a_m = m\pi/2a$. To determine the unknown coefficient c_m it is necessary to match the boundary conditions of tangential E- and H-field continuities. From the tangential E-field and H-field continuities at $z = d_2 = d_1 + b$, we obtain

$$\tilde{H}_{II}^{-}(\zeta) = e^{i2\kappa_2 d_2}\left(\frac{\epsilon_1\kappa_2 - \epsilon_2\kappa_1}{\epsilon_1\kappa_2 + \epsilon_2\kappa_1}\right)\tilde{H}_{II}^{+}(\zeta) \tag{6}$$

Similarly, the tangential E-field and H-field continuities at $z = d_1$ yield

$$\tilde{H}_{III}^{-}(\zeta) = \left[\frac{(\epsilon_2\kappa_3 - \epsilon_3\kappa_2)(\epsilon_1\kappa_2 + \epsilon_2\kappa_1)e^{2i\kappa_2 d_1} + (\epsilon_2\kappa_3 + \epsilon_3\kappa_2)(\epsilon_1\kappa_2 - \epsilon_2\kappa_1)e^{2i\kappa_2 d_2}}{(\epsilon_2\kappa_3 + \epsilon_3\kappa_2)(\epsilon_1\kappa_2 + \epsilon_2\kappa_1)e^{2i\kappa_2 d_1} + (\epsilon_2\kappa_3 - \epsilon_3\kappa_2)(\epsilon_1\kappa_2 - \epsilon_2\kappa_1)e^{2i\kappa_2 d_2}}\right] \cdot e^{i2\kappa_3 d_1}\tilde{H}_{III}^{+}(\zeta) \equiv \left(\frac{\alpha_1}{\alpha_2}\right)\tilde{H}_{III}^{+}(\zeta) \tag{7}$$

IEE Proceedings online no. 19960444

Paper first received 11th September 1995 and in revised form 8th March 1996

The authors are with the Department of Electrical Engineering, Korea Advanced Institute of Science and Technology, 373-1, Kusong Dong, Yusung Gu, Taejon, Korea

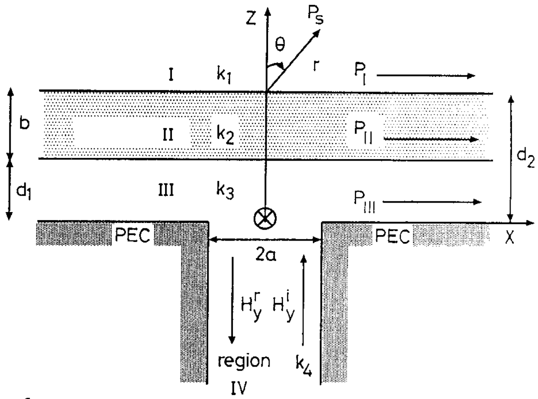

Fig. 1 *Scattering geometry*

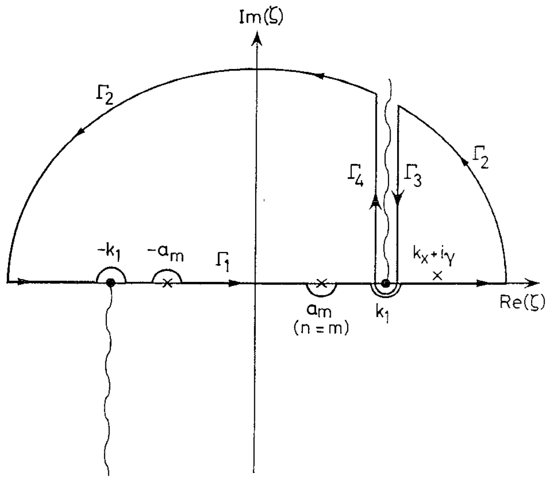

Fig. 2 *Closed path for contour integration in ζ-plane*

The tangential E-field continuity at $z = 0$ and eqn. 7 yield

$$\tilde{H}^{+}_{III}(\zeta)\left(1-\frac{\alpha_1}{\alpha_2}\right)=\frac{1}{\kappa_3}\left[\xi_p K_p(\zeta)-\sum_{m=0}^{\infty} c_m \xi_m K_m(\zeta)\right]\frac{\epsilon_3}{\epsilon_4} \tag{8}$$

where

$$K_m(\zeta)=\frac{\zeta}{i(\zeta^2-a_m^2)}[e^{i\zeta a}(-1)^m-e^{-i\zeta a}] \tag{9}$$

Substituting eqn. 8 into the tangential H-field continuity along the aperture ($-a < x < a$, $z = 0$) and some algebraic manipulation obtains

$$\frac{\epsilon_3}{2\pi\epsilon_4}\left[\xi_p I_{np}-\sum_{m=0}^{\infty} c_m \xi_m I_{nm}\right]=\varepsilon_n a\delta_{np}+\varepsilon_n c_n a \tag{10}$$

where δ_{np} represents the Kronecker delta, $\varepsilon_0 = 2$, $\varepsilon_1 = \varepsilon_2 = \ldots = 1$, and

$$I_{nm}=\int_{-\infty}^{\infty}\left[\frac{\alpha_2+\alpha_1}{\kappa_3(\alpha_2-\alpha_1)}\right]K_m(\zeta)K_n(-\zeta)d\zeta \tag{11}$$

The analytic contour integration of I_{mn} is performed in Section 7.1 to give

$$I_{nm}=\varepsilon_m h_m \delta_{nm}+l_{nm}-r_{nm} \tag{12}$$

where h_m is a residue contribution at $\zeta = \pm a_m$ and l_{nm} represents a residue contribution at $\zeta = k_x$ which is a zero of $(\alpha_2 - \alpha_1)$. r_{nm} is a branch-cut integration associated with a branch point at $\zeta = k_1$ (Fig. 2). From eqns. 10 and 12 we obtain c_n in rapidly converging series as

$$C=(U-T)^{-1}Q \tag{13}$$

where U is the identity matrix and the elements of matrices T and Q are

$$t_{nm}=-\frac{\xi_m\epsilon_3(l_{nm}-r_{nm})}{(\xi_n h_n\epsilon_3+2\pi a\epsilon_4)\varepsilon_n} \tag{14}$$

$$q_n=\frac{\varepsilon_p\epsilon_3 h_p\xi_p-2\pi\varepsilon_n a\epsilon_4}{(\xi_n h_n\epsilon_3+2\pi a\epsilon_4)\varepsilon_n}\delta_{np}+\frac{\epsilon_3\xi_p(l_{np}-r_{np})}{(\xi_n h_n\epsilon_3+2\pi a\epsilon_4)\varepsilon_n} \tag{15}$$

When $2a < 0.5\lambda_4$, a single-mode approximation is applicable where eqn. 13 becomes $c_n \simeq 0$, $n \geq 1$,

$$c_0=\frac{1-2\pi\varepsilon_0 a\epsilon_4/[\varepsilon_0\epsilon_3 h_0\xi_0+\xi_0\epsilon_3(l_{00}-r_{00})]}{1+2\pi\varepsilon_0 a\epsilon_4/[\varepsilon_0\epsilon_3 h_0\xi_0+\xi_0\epsilon_3(l_{00}-r_{00})]} \tag{16}$$

3 Numerical computations

The far-zone radiation field and power in region I are

$$H_y^s(r,\theta)=\sqrt{\frac{k_1}{2\pi r}}e^{i(\kappa_2 d_2+k_1 r-\frac{\pi}{4})}2\epsilon_1\frac{\kappa_2}{\kappa_3}\cos\theta_s\Lambda \cdot\left[\xi_p K_p(\zeta)-\sum_{m=0}^{\infty}c_m\xi_m K_m(\zeta)\right]\Bigg|_{\zeta=-k_1\sin\theta} \tag{17}$$

$$\sigma=P_s/P_i=\frac{k_1}{\xi_p\varepsilon_p a}\int_{-\frac{\pi}{2}}^{\frac{\pi}{2}}\left|H_y^s(r,\theta)\right|^2 r\,d\theta \tag{18}$$

where

$$\Lambda=\left[\left\{-i\epsilon_3\epsilon_1\frac{\xi}{\cos\theta}\cos(k_1 d_1\cos\theta)-\epsilon_2\epsilon_2\frac{\cos\theta}{\xi}\sin(k_1 d_1\cos\theta)\right\}\cdot\sin(k_1 b\xi)+e^{-ik_1 d_1\cos\theta}\epsilon_3\epsilon_2\cos(k_1 b\xi)\right]^{-1} \tag{19}$$

which is identical with eqn. 19 in [6] and $\xi = \surd[(\epsilon_2/\epsilon_1) - \sin^2\theta]$. Λ becomes maximum at angles given by either $d_1\cos\theta = m\lambda_3/2$, $b\surd[(\epsilon_2/\epsilon_1) - \sin^2\theta] = (2n-1)\lambda_4/4$ or $d_1\cos\theta = (2m-1)\lambda_3/4$, $b\surd[(\epsilon_2/\epsilon_1) - \sin^2\theta] = n\lambda_4/2$. The reflected and transmitted powers associated with surface waves in regions I, II, and III are

$$\rho=P_r/P_i=\frac{1}{\xi_p\varepsilon_p}\sum_m\xi_m\varepsilon_m|c_m|^2,\quad 0\le m<\frac{k_4 2a}{\pi} \tag{20}$$

$$\tau_1=\frac{P_I}{P_i}=\frac{k_x\epsilon_4}{\epsilon_1\xi_p\varepsilon_p a}\left[\frac{1}{2k_{z1}}e^{-2k_{z1}d_2}\right]|K_I|^2 \tag{21}$$

$$\begin{aligned}\tau_2&=P_{II}/P_i\\&=\frac{k_x\epsilon_4}{2\epsilon_2\xi_p\varepsilon_p a}\Bigg[|K_{II}^c|^2 b+|K_{II}^c|^2\frac{[\sin(2k_{z2}d_2)-\sin(2k_{z2}d_1)]}{2k_{z2}}\\&\quad+|K_{II}^s|^2 b-|K_{II}^s|^2\frac{[\sin(2k_{z2}d_2)-\sin(2k_{z2}d_1)]}{2k_{z2}}\Bigg]\\&\quad-\frac{k_x\epsilon_4}{4\xi_p\epsilon_2\varepsilon_p k_{z2}a}(\cos k_{z2}d_2-\cos k_{z2}d_1)\\&\quad\times\mathrm{Re}\{K_{II}^c(K_{II}^s)^*+K_{II}^s(K_{II}^c)^*\}\end{aligned} \tag{22}$$

$$\begin{aligned}\tau_3&=P_{III}/P_i\\&=\frac{k_x\epsilon_4}{2\epsilon_3\xi_p\varepsilon_p a}\left[|K_{III}^c|^2 d_1-|K_{III}^c|^2\frac{1}{2k_{z3}}\sinh 2k_{z3}d_1\right.\\&\quad\left.+|K_{III}^s|^2 d_1+|K_{III}^s|^2\frac{1}{2k_{z3}}\sinh 2k_{z3}d_1\right]\\&\quad-\frac{k_x\epsilon_4}{4\xi_p\epsilon_3\varepsilon_p k_{z3}a}(2+2\cosh(2k_{z3}d_1))\\&\quad\times\mathrm{Re}\{iK_{III}^c(K_{III}^s)^*-iK_{III}^s(K_{III}^c)^*\}\end{aligned} \tag{23}$$

where $k_{z1} = \sqrt{[k_x^2 - k_1^2]}$, $k_{z2} = \sqrt{[k_2^2 - k_x^2]}$, $k_{z3} = \sqrt{[k_x^2 - k_3^2]}$ and K_I, $K_{II}^{c,s}$, $K_{III}^{c,s}$ are given in Section 7.2, and * denotes the complex conjugate. The power conservation requires $\sigma + \tau_1 + \tau_2 + \tau_3 + \rho = 1$. We compare our results of $\sqrt{\rho}$ with [5] in Fig. 3, thereby confirming a good agreement when eqn. 16 is used. The number of modes m used in our computation is one (i.e. $m = 0$), which implies no matrix operation is required when $2a < 0.5\lambda_4$. Fig. 4 illustrates the angular radiation pattern for different b, showing the maximum radiation at $\theta = 0°$ occurs when $b\sqrt{[(\epsilon_2/\epsilon_1)]} = (2n - 1)\lambda_4/4$. When a flanged rectangular waveguide of dimension ($h \times 2a$, $h > 2a$) is excited with the TE_{10} mode, it is possible to apply our solution eqn. 16 to the rectangular waveguide problem by replacing k_4 in eqns. 4 and 5 with $k_g = \sqrt{[k_4^2 - (\pi/h)^2]}$. In Fig. 5, we consider a flanged rectangular waveguide radiating into a dielectric slab with a different slab thickness b. Fig. 5 illustrates that our simple solution agrees well with [7] when $b = 0$. As d_1 increases, the oscillating amplitude of $\sqrt{\rho}$ becomes less pronounced, thereby approaching 0.42 which is the reflection coefficient when $\epsilon_1 = \epsilon_2 = \epsilon_3 = 2.59$ and $\epsilon_4 = 1$.

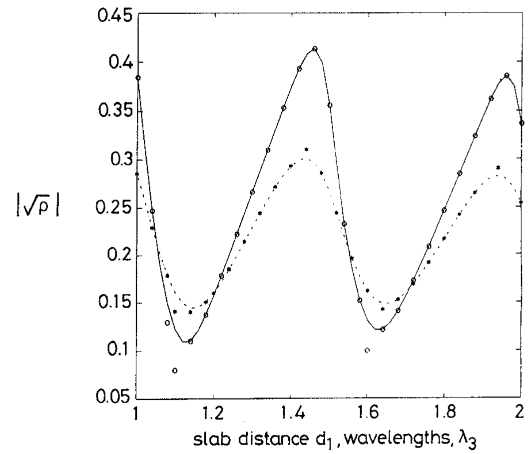

Fig. 3 *Reflection coefficient of TEM wave against slab distance*
$a = 0.2\lambda_4$, $\epsilon_1 = \epsilon_3 = \epsilon_4 = 1$; $\epsilon_2 = 4$
——— $b = 0.75\lambda_2$
– · – $b = \infty$
✳ Fig. 11 in [5]
○ Fig. 11 in [5]

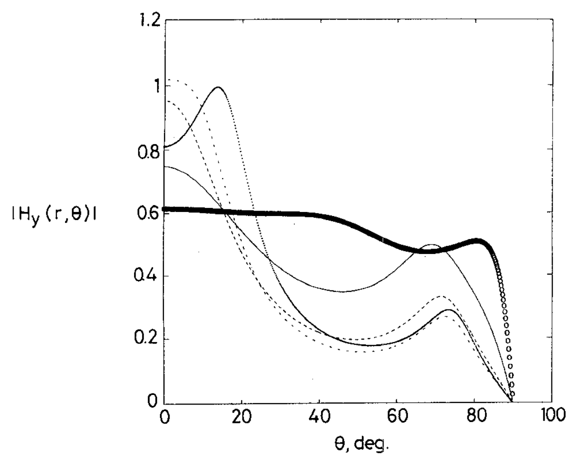

Fig. 4 *Radiation pattern against slab thickness b*
$\epsilon_1 = \epsilon_3 = \epsilon_4 = 1$; $\epsilon_2 = 9$; $d_1 = 0.5\lambda_3$; $a = 0.2\lambda_4$
——— $b = 0.1\lambda_2$
– – – $b = 0.2\lambda_2$
– · – $b = 0.25\lambda_2$
······ $b = 0.3\lambda_2$
○○○○○○ $b = 0.5\lambda_2$

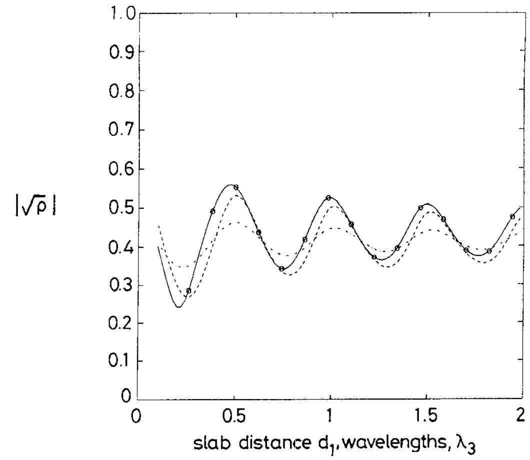

Fig. 5 *Reflection coefficient (TE_{10} mode) of rectangular waveguide against slab distance d_1/λ_3*
$\epsilon_1 = 8.9$, $\epsilon_2 = 6$, $\epsilon_3 = 2.59$; $\epsilon_4 = 1$ at 10GHz
——— $b = 0$
○ Fig. 2 in [7]
– · – $b = 0.25\lambda_2$
– – – $b = 0.5\lambda_2$

4 Conclusion

TM-wave radiation from a flanged parallel plate into a dielectric slab has been studied using the Fourier transform and mode matching. A rapidly converging series solution which is suitable for numerical computation was obtained and simple condition for predicting a maximum radiation angle presented. Our single-mode approximate solution predicts well radiation of a flanged rectangular waveguide of the TE_{10} mode.

5 Acknowledgments

This research was supported in parts by the Korea Telecom Research Center (contract GI26760), the KOSEF (contract NL04161), and IITA (contract NN16020).

6 References

1 JONES, J.E.: 'The influence of air-gap tolerances on the admittance of a dielectric coated slot antenna', *IEEE Trans.*, Jan. 1969, **AP-17**, (1), pp. 63–68
2 WU, C.P.: 'Integral equation solutions for the radiation from a waveguide through a dielectric slab', *IEEE Trans.*, Nov. 1969, **AP-17**, (6), pp. 733–739
3 CROSWELL, W.F., RUDDUCK, R.G., and HATCHER, D.M.: 'The admittance of a rectangular waveguide radiating into a dielectric layer', *IEEE Trans.*, Sept. 1967, **AP-15**, (5)
4 GALEJS, J., 'Antennas in inhomogeneous media' (Pergamon, 1969, 1st edn.), pp. 104–119
5 BURNSIDE, W.D., RUDDUCK, R.C., TSAI, L.L., and JONES, J.E.: 'Reflection coefficient of a TEM mode symmetric parallel-plate waveguide illuminating a dielectric layer', *Radio Sci.*, June 1969, **4**, (6), pp. 545–556
6 SUGIO, Y., MAKIMOTO, T., and TSUGAWA, T.: 'Two dimensional-analysis for gain enhancement of dielectric loaded antenna with a ground plane', *Trans. IEICE Japan*, Aug. 1990, **J73-B-II**, (8), pp. 405–412
7 GENTILI, G.B., MANARA, G., PELOSI, G., and TIBERIO, R.: 'Radiation of open-ended waveguides into stratified media', *Microw. Opt. Technol. Lett.*, Sept. 1991, **4**, (10) pp. 401–403

7 Appendix

7.1 Evaluation of integral I_{nm}

When $m + n$ is odd, $I_{nm} = 0$. When $m + n$ is even, I_{nm} is

$$I_{nm} = \int_{-\infty}^{\infty} 2\left(\frac{\alpha_2 + \alpha_1}{\alpha_2 - \alpha_1}\right) \frac{\zeta^2[1 - (-1)^m e^{i2\zeta a}]}{(\zeta^2 - a_m^2)(\zeta^2 - a_n^2)\kappa_3} d\zeta \quad (24)$$

We assume that ϵ_2 has a small positive imaginary part for analytic convenience. Integrating along the deformed contour Γ_1, Γ_2, Γ_3, and Γ_4 in the upper half-plane in Fig. 2, obtains

$$I_{nm} = \varepsilon_m h_m \delta_{nm} - r_{nm} + l_{nm}$$

where δ_{nm} is the Kronecker delta,

$$h_m = 2\pi a/\sqrt{k_3^2 - a_m^2}\left(\frac{\alpha_2+\alpha_1}{\alpha_2-\alpha_1}\right)\Bigg|_{\zeta=a_m}$$

$$l_{nm} = \sum_{k_x} \frac{4\pi i\zeta^2(\alpha_2+\alpha_1)[1-(-1)^m e^{i2k_x a}]}{(\alpha_2-\alpha_1)'(\zeta^2-a_m^2)(\zeta^2-a_n^2)\kappa_3}\Bigg|_{\zeta=k_x}$$

and (...)′ denotes the differentiation with respect to ζ. The branch-cut contribution r_{nm} along Γ_3 and Γ_4 is

$$r_{nm} = \int_0^\infty dv \frac{2i[1-(-1)^m e^{i2ak_1} e^{-2ak_1 v}](1+iv)^2}{k_1[(1+iv)^2-(a_m/k_1)^2][(1+iv)^2-(a_n/k_1)^2]\sqrt{k_3^2-k_1^2(1+iv)^2}} f(v) \tag{25}$$

where

$$f(v) = -\left(\frac{\alpha_2+\alpha_1}{\alpha_2-\alpha_1}\right)\Bigg|_{\kappa_1\to-\kappa_1,\zeta=k_1+ik_1v} + \left(\frac{\alpha_2+\alpha_1}{\alpha_2-\alpha_1}\right)\Bigg|_{\zeta=k_1+ik_1v}$$

7.2

$$K_I = -2iAe^{i(k_{z2}-ik_{z1})d_2}\epsilon_1 k_{z2} \tag{26}$$

$$K_{II}^c = -2iAe^{ik_{z2}d_2}[\epsilon_1 k_{z2}\cos(k_{z2}d_2)+\epsilon_2 k_{z1}\sin(k_{z2}d_2)]e^{k_{z3}d_1} \tag{27}$$

$$K_{II}^s = -2iAe^{ik_{z2}d_2}[\epsilon_1 k_{z2}\sin(k_{z2}d_2)-\epsilon_2 k_{z1}\cos(k_{z2}d_2)]e^{k_{z3}d_1} \tag{28}$$

$$\begin{aligned}K_{III}^c =& 2Be^{-k_{z3}d_1}\epsilon_2 k_{z3}[i\epsilon_2 k_{z1}(e^{i2k_{z2}d_1} - e^{i2k_{z2}d_2}) \\ &+ \epsilon_1 k_{z2}(e^{i2k_{z2}d_1} + e^{i2k_{z2}d_2})]\end{aligned} \tag{29}$$

$$\begin{aligned}K_{III}^s =& 2Be^{-k_{z3}d_1}\epsilon_3 k_{z2}[\epsilon_1 k_{z2}(e^{i2k_{z2}d_1} - e^{i2k_{z2}d_2}) \\ &+ i\epsilon_2 k_{z1}(e^{i2k_{z2}d_1} + e^{i2k_{z2}d_2})]\end{aligned} \tag{30}$$

$$A = \frac{(\epsilon_3/\epsilon_4)[\xi_p K_p(\zeta) - \sum_{m=0}^{\infty} c_m \xi_m K_m(\zeta)][\alpha_2 e^{i\kappa_3 d_1} + \alpha_1 e^{-i\kappa_3 d_1}]}{\kappa_3[e^{i\kappa_2 d_1}(\epsilon_1\kappa_2+\epsilon_2\kappa_1)+e^{i2\kappa_2 d_2 - i\kappa_2 d_1}(\epsilon_1\kappa_2-\epsilon_2\kappa_1)][(\alpha_2-\alpha_1)e^{-i\kappa_3 d_1}]'}\Bigg|_{\zeta=-k_x} \tag{31}$$

$$B = \frac{[\xi_p K_p(\zeta) - \sum_{m=0}^{\infty} c_m \xi_m K_m(\zeta)](\epsilon_3/\epsilon_4)}{[\alpha_2-\alpha_1]'\kappa_3}\Bigg|_{\zeta=-k_x} \tag{32}$$